PROCEEDINGS OF SCIENCE

Chebyshev and Backus-Gilbert reconstruction for inclusive semileptonic $B_{(s)}$-meson decays from Lattice QCD

Alessandro Barone,[a,b,c,*] **Shoji Hashimoto,**[e,f] **Andreas Jüttner,**[b,c,d] **Takashi Kaneko**[e,f,g] **and Ryan Kellermann**[e,f]

[a] *PRISMA+ Cluster of Excellence & Institut für Kernphysik, Johannes-Gutenberg-Universität Mainz, D-55099 Mainz, Germany*

[b] *School of Physics and Astronomy, University of Southampton, Southampton SO17 1BJ, UK*

[c] *STAG Research Center, University of Southampton, Southampton SO17 1BJ, UK*

[d] *CERN, Theoretical Physics Department, Geneva, Switzerland*

[e] *High Energy Accelerator Research Organization (KEK), Ibaraki 305-0801, Japan*

[f] *School of High Energy Accelerator Science, SOKENDAI (The Graduate University for Advanced Studies), Ibaraki 305-0801, Japan*

[g] *Kobayashi-Maskawa Institute for the Origin of Particles and the Universe, Nagoya University, Aichi 464–8602, Japan*

E-mail: abarone@uni-mainz.de

We present a study on the nonperturbative calculation of observables for inclusive semileptonic decays of $B_{(s)}$ mesons using lattice QCD. We focus on the comparison of two different methods to analyse the lattice data of Euclidean correlation functions, specifically Chebyshev and Backus-Gilbert approaches. This type of computation may eventually provide new insight into the long-standing tension between the inclusive and exclusive determinations of the Cabibbo-Kobayashi-Maskawa (CKM) matrix elements $|V_{cb}|$ and $|V_{ub}|$. We report the results from a pilot lattice computation for the decay $B_s \to X_c\, l \nu_l$, where the valence quark masses are approximately tuned to their physical values using the relativistic-heavy quark action for the b quark and the domain-wall formalism for the other valence quarks. We address the computation of the total decay rate as well as leptonic and hadronic moments, discussing similarities and differences between the two analysis techniques.

The 40th International Symposium on Lattice Field Theory (Lattice 2023)
July 31st - August 4th, 2023
Fermi National Accelerator Laboratory

*Speaker

© Copyright owned by the author(s) under the terms of the Creative Commons Attribution-NonCommercial-NoDerivatives 4.0 International License (CC BY-NC-ND 4.0).

PoS(LATTICE2023)236

1. Introduction

Quark-flavour physics is an area of particular interest to search for deviation from the Standard Model (SM), as weak processes characterised by flavour-changing currents may be sensitive to New Physics: while new particles may be too heavy to be produced with energies achievable by current experimental facilities, quantum effects could leave detectable traces in flavour-physics processes. Therefore, any discrepancy between SM theoretical predictions and experimental measurements could be an indicator of new effects.

One intriguing puzzle is the long-standing tension between the inclusive and exclusive determinations of the Cabibbo-Kobayashi-Maskawa (CKM) matrix elements $|V_{cb}|$ and $|V_{ub}|$. Semileptonic decays of B mesons constitute the main channel for the extraction of these parameters, and therefore represent crucial processes to address and investigate this tension.

First viable theoretical proposals for how to accomplish the computation of inclusive decay observables on the lattice have appeared only recently [1–3]. We report on our pilot study on the calculation of the decay rate of the inclusive semileptonic $B_s \to X_c\, l \nu_l$ decay [4, 5], focusing on similarities and differences of the analysis strategy based on the Chebyshev polynomial and Backus-Gilbert reconstruction. We present further work on the generalisation of our setup to the computation of moments of various kinematical quantities, in particular hadronic mass and lepton energy moments.

2. Inclusive decay rate and kinematic moments

The starting point of the calculation is given by the differential decay rate

$$\frac{\mathrm{d}\Gamma}{\mathrm{d}q^2 \mathrm{d}q_0 \mathrm{d}E_l} = \frac{G_F^2 |V_{cb}|^2}{8\pi^3} L_{\mu\nu} W^{\mu\nu} \,, \tag{1}$$

where $W^{\mu\nu} \equiv W^{\mu\nu}(p,q)$ is the hadronic tensor for the B_s decay defined as

$$W^{\mu\nu} = \sum_{X_c} (2\pi)^3 \delta^{(4)}(p-q-r) \frac{1}{2E_{B_s}(\boldsymbol{p})} \langle B_s(\boldsymbol{p})| J^{\mu\dagger}(0) |X_c(\boldsymbol{r})\rangle \langle X_c(\boldsymbol{r})| J^{\nu}(0) |B_s(\boldsymbol{p})\rangle \,, \tag{2}$$

which contains all the nonperturbative QCD effects, and $L^{\mu\nu}$ is the leptonic tensor which contains known kinematic terms associated with the lepton-neutrino pair.

The total decay rate is obtained integrating Eq. (1)

$$\Gamma = \frac{G_F^2 |V_{cb}|^2}{24\pi^3} \int_0^{\boldsymbol{q}^2_{\max}} \mathrm{d}\boldsymbol{q}^2 \sqrt{\boldsymbol{q}^2}\, \bar{X}(\boldsymbol{q}^2) \,, \tag{3}$$

where we changed the integration variables to the three-momentum $\boldsymbol{q}^2$ of the hadronic state X_c and its energy ω, with

$$\bar{X}(\boldsymbol{q}^2) \equiv \frac{3}{\sqrt{\boldsymbol{q}^2}} \int_{\omega_0}^{\infty} \mathrm{d}\omega \int_{E_l^{\min}}^{E_l^{\max}} \mathrm{d}E_l L_{\mu\nu} W^{\mu\nu} = \int_{\omega_0}^{\infty} \mathrm{d}\omega\, K_{\mu\nu} W^{\mu\nu} \,, \tag{4}$$

where $K_{\mu\nu} = K_{\mu\nu}(\boldsymbol{q}^2, \omega)$ is a kernel function that contains known kinematic factors obtained from the leptonic tensor after the integration over the lepton energy E_l. While the energy phase space

PoS(LATTICE2023)236

in ω is restricted in some finite interval $\omega \in [\omega_{\min}, \omega_{\max}]$ for every $\boldsymbol{q}^2$, we are free to modify the integration range to $\omega_0 \leq \omega_{\min}$, since the hadronic tensor has no support below the ground state $\omega_{\min}$, and extend $\omega_{\max} \to \infty$ including a Heaviside function into the kernel $K_{\mu\nu}$. These modifications will be relevant later for the analysis strategy.

Moving to the moments of a given kinematic quantity p at order n, these are defined as

$$\langle (p)^n \rangle = \frac{\Gamma_{p_n}}{\Gamma}, \quad \Gamma_{p_n} \equiv \int \mathrm{d}\boldsymbol{q}^2 \mathrm{d}\omega \mathrm{d}E_l \, (p)^n \left[\frac{\mathrm{d}\Gamma}{\mathrm{d}\boldsymbol{q}^2 \, \mathrm{d}\omega \, \mathrm{d}E_l} \right], \tag{5}$$

which can be rewritten as

$$\langle (p)^n \rangle = \frac{\int \mathrm{d}\boldsymbol{q}^2 \sqrt{\boldsymbol{q}^2} \bar{X}_p^{(n)}(\boldsymbol{q}^2)}{\int \mathrm{d}\boldsymbol{q}^2 \sqrt{\boldsymbol{q}^2} \bar{X}(\boldsymbol{q}^2)}, \tag{6}$$

with

$$\bar{X}_p^{(n)}(\boldsymbol{q}^2) = \frac{3}{\sqrt{\boldsymbol{q}^2}} \int_{\omega_0}^{\infty} \mathrm{d}\omega \int_{E_l^{\min}}^{E_l^{\max}} \mathrm{d}E_l \, (p)^n L_{\mu\nu} W^{\mu\nu} = \int_{\omega_0}^{\infty} \mathrm{d}\omega \, K_{p,\mu\nu}^{(n)} W^{\mu\nu}, \tag{7}$$

where $K_{p,\mu\nu}^{(n)}$ is the corresponding kernel function analogous to the one in Eq. (4). We consider in particular the hadronic mass (H) moments $\langle (M_X^2)^n \rangle$, with $M_X^2 = (\omega^2 - \boldsymbol{q}^2)$, and the lepton energy (L) moments $\langle (E_l)^n \rangle$. In order to discuss and illustrate our method, we will focus on the computation of $\bar{X}(\boldsymbol{q}^2)$ and the analogous quantities for the $n = 1$ moments $\bar{X}_H^{(1)}(\boldsymbol{q}^2)$ and $\bar{X}_L^{(1)}(\boldsymbol{q}^2)$, which are the crucial ingredients to compute the final observables of interest.

3. Lattice approach

Inclusive decays can be studied on the lattice through the computation of four-point correlation functions

$$C_{\mu\nu}^{SJJS}(t_{\mathrm{snk}}, t_2, t_1, t_{\mathrm{src}}) = \sum_{\boldsymbol{x}_{\mathrm{snk}}} e^{-i\boldsymbol{p}_{\mathrm{snk}} \cdot (\boldsymbol{x}_{\mathrm{snk}} - \boldsymbol{x}_{\mathrm{src}})} \left\langle T \left\{ O_{B_s}^S(x_{\mathrm{snk}}) \, \tilde{J}_\mu^\dagger(\boldsymbol{q}, t_2) \, \tilde{J}_\nu(\boldsymbol{q}, t_1) \, O_{B_s}^{S\dagger}(x_{\mathrm{src}}) \right\} \right\rangle, \tag{8}$$

where O_{B_s} is an interpolating operator for the the B_s meson, and $\tilde{J}_\nu$ is the $\bar{b} \to \bar{c}$ weak current projected in momentum space. In particular, the hadronic tensor can be addressed through the ratio

$$C_{\mu\nu}(\boldsymbol{q}, t) \equiv \frac{1}{2M_{B_s}} |\langle 0| O_{B_s}^L |B_s\rangle|^2 \frac{C^{SJJS}(t_{\mathrm{snk}}, t_2, t_1, t_{\mathrm{src}})}{C^{SL}(t_{\mathrm{snk}}, t_2) C^{LS}(t_1, t_{\mathrm{src}})}, \tag{9}$$

with $t_{\mathrm{snk}} - t_2 \gg 1$, $t_1 - t_{\mathrm{src}} \gg 1$ and $t = t_2 - t_1$, and where C^{XY} represent the two-point B_s correlator, with the superscripts indicating smearing (S) or no smearing (L). Indeed, the new correlator $C_{\mu\nu}(\boldsymbol{q}, t)$ is related to the hadronic tensor as

$$C_{\mu\nu}(\boldsymbol{q}, t) = \int_{\omega_0}^{\infty} \mathrm{d}\omega \, W_{\mu\nu}(\boldsymbol{q}, \omega) e^{-\omega t}, \tag{10}$$

PoS(LATTICE2023)236

which shows that $W_{\mu\nu}$ represents the spectral function for the correlator $C_{\mu\nu}$ in the Källén-Lehmann representation, namely

$$W_{\mu\nu}(\boldsymbol{q},\omega) = \frac{1}{2M_{B_s}} \sum_{X_c} \delta(\omega - E_{X_c}) \langle B_s | \tilde{J}^{\dagger}_{\mu}(\boldsymbol{q},0) | X_c \rangle \langle X_c | \tilde{J}_{\nu}(\boldsymbol{q},0) | B_s \rangle \tag{11}$$

in the rest frame of the B_s meson.

The extraction of the hadronic tensor requires the computation of the inverse Laplace transform and represents therefore an ill-posed inverse problem. However, for the calculation of the quantities $\bar{X}(\boldsymbol{q}^2)$ for both decay rate and moments the extraction of the spectral function can be bypassed and the observables can be evaluated directly. In particular, referring to Eqs. (4) and (7), $\bar{X}(\boldsymbol{q}^2)$ can be obtained naively through a polynomial approximation in $e^{-\omega}$ (in lattice units) of the kernel function up to a degree N, i.e. $K_{\mu\nu} = \sum_{j=0}^{N} c_{\mu\nu,j} e^{-j\omega}$ such that

$$\bar{X}_{\text{naive}}(\boldsymbol{q}^2) = \sum_{j=0}^{N} c_{\mu\nu,j} \int_{\omega_0}^{\infty} \mathrm{d}\omega \, W^{\mu\nu} e^{-j\omega} = \sum_{j=0}^{N} c_{\mu\nu,j} C^{\mu\nu}(j) \, . \tag{12}$$

Note that the approximation of the kernel is possible as long as the Heaviside function contained in $K_{\mu\nu}$ is regularised with a continuous function such as a sigmoid $\theta_\sigma(x) = 1/(1+e^{-x/\sigma})$, where σ is a parameter that controls the sharpness of the step and approaches the Heaviside for $\sigma \to 0$. While this observation plays an important role in the final calculation, we won't discuss it further and refer to other works for more details [5, 6]. We labelled the above calculation as "naive" because, while theoretically well-defined, such a procedure would in practice lead to a build up of the statistical noise originating from the correlator at different time slices, such that the final error on $\bar{X}_{\text{naive}}(\boldsymbol{q}^2)$ would be too large to make any significant phenomenological prediction. To proceed in the analysis we then need to consider two steps:

1. find a suitable polynomial approximation strategy to approximate the kernels;
2. devise a "regularisation" to reduce the variance of the target observable.

The final result for the observable is then

$$\bar{X}(\boldsymbol{q}^2) = \bar{X}_{\text{naive}}(\boldsymbol{q}^2) + \delta\bar{X}(\boldsymbol{q}^2) \, , \tag{13}$$

where $\delta\bar{X}(\boldsymbol{q}^2)$ is the regularisation term which acts as a noisy zero that does not change the final result but takes care of reducing the variance.

4. Chebyshev and Backus-Gilbert reconstruction

For the analysis strategy we rely on polynomial approximations based on the Chebyshev polynomial technique [7, 8] and the Backus-Gilbert method [9, 10]. We refer to the App. of [5] for a deeper discussion of both approaches. Here we point out the main differences between the two in terms of the polynomial approximation of the kernels (with no connection to the data) as well as the variance reduction of the final $\bar{X}(\boldsymbol{q}^2)$ observables.

PoS(LATTICE2023)236

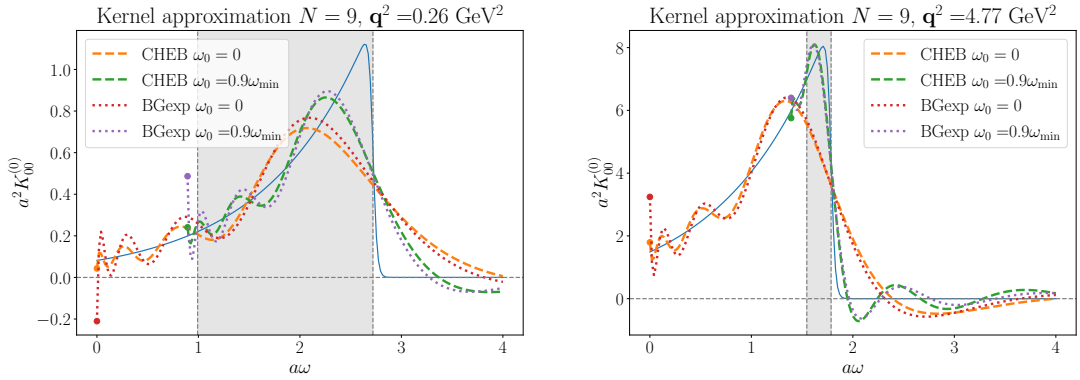

Figure 1: Example of the polynomial approximation of one of the kernels for the decay rate at degree $N = 9$ with Chebyshev and Backus-Gilbert method with two different starting point ω_0 for the polynomial approximation.

Let us start from the polynomial approximation. We first highlight that, by visual inspection of Fig. 1, the quality of the two polynomial approximation strategies is comparable. Furthermore, the choice of the starting point of the approximation ω_0 (cf. with the integral in (4)) has a significant impact on the quality of the reconstruction, in particular for larger $\boldsymbol{q}^2$, where the phase space in ω is shrunk (right plot).

Concerning the variance reduction, the two methods act in a significantly different way. The Chebyshev-polynomial technique relies on trading the original data with a refitted set that accounts for rigorous mathematical bounds associated with the shifted Chebyshev polynomials $\tilde{T}_j(\omega)$, $\omega \in [\omega_0, \infty)$, for which $|\tilde{T}_j(\omega)| \leq 1$. Namely, the normalised correlator in Eq. (9) can be written as linear combination of $\tilde{T}_{j,\mu\nu} \equiv \left(\int_{\omega_0}^{\infty} \mathrm{d}\omega W_{\mu\nu} \tilde{T}_j(\omega) e^{-2t_0\omega}\right) / \left(\int_{\omega_0}^{\infty} \mathrm{d}\omega W_{\mu\nu} \tilde{T}_0(\omega) e^{-2t_0\omega}\right)$, such that we can obtain a new set of data for the normalised correlator $\bar{C}_{\mu\nu}(\boldsymbol{q}, j) = C_{\mu\nu}(\boldsymbol{q}, j + 2t_0)/C_{\mu\nu}(\boldsymbol{q}, 2t_0)$ requiring

$$\bar{C}^{\text{fit}}_{\mu\nu}(\boldsymbol{q}, k) = \sum_{j=0}^{k} \tilde{a}_j^{(k)} \tilde{T}_{j,\mu\nu}\,, \tag{14}$$

and imposing the bounds $|\tilde{T}_{j,\mu\nu}| \leq 1$ in the fitting procedure, where $\tilde{a}_j^{(k)}$ is a set of known coefficients associated with the power representation of the polynomials. The shift t_0 represents the minimum distance between the two currents in Eq. (8) and has to be accounted for in $K_{\mu\nu}$. In this way, the correction term reads

$$\delta\bar{X}(\boldsymbol{q}^2) = C_{\mu\nu}(\boldsymbol{q}, 2t_0) \sum_{j=0}^{N} c_{\mu\nu,j}\, \delta\bar{C}_{\mu\nu}(\boldsymbol{q}, j)\,, \quad \delta\bar{C}_{\mu\nu}(\boldsymbol{q}, j) = \bar{C}^{\text{fit}}_{\mu\nu}(\boldsymbol{q}, j) - \bar{C}_{\mu\nu}(\boldsymbol{q}, j) \tag{15}$$

and the variance is minimised acting of the correlator data.

On the other hand, the Backus-Gilbert method reduces the variance by modifying the coefficients of the polynomial approximation such that they account also for the reduction of the statistical noise. This is achieved in practice by minimising the functional

$$F = A + \theta^2 B\,, \tag{16}$$

PoS(LATTICE2023)236

where the functional A addresses the pure polynomial approximation (systematic error) with a chosen polynomial basis $b_j(\omega)$, B addresses the variance of $\bar{X}(\boldsymbol{q}^2)$ (statistical error) and θ^2 is a parameter chosen by hand that accounts for the interplay between the two types of error. The "naive" result is then regularised through a correction to the coefficients as

$$\delta\bar{X}(\boldsymbol{q}^2) = C_{\mu\nu}(\boldsymbol{q}, 2t_0) \sum_{j=0}^{N} \delta c_{\mu\nu,j}\, \bar{C}_{\mu\nu}(\boldsymbol{q}, j)\,, \quad \delta c_{\mu\nu,j} = \delta c_{\mu\nu,j}\Big|_{\theta^2\neq 0} - \delta c_{\mu\nu,j}\Big|_{\theta^2=0}\,. \tag{17}$$

5. Numerical setup

Our calculation is based on a $24^3\times 64$ lattice with 2+1-flavour domain-wall fermion (DWF) [11, 12] gauge-field ensembles with the Iwasaki gauge action [13] from the RBC/UKQCD Collaboration [14] at lattice spacing $a^{-1} = 1.785(5)$ GeV (corresponding to $a \simeq 0.11$ fm), pion mass $M_\pi \simeq 340$ MeV and close-to-physical strange-quark mass. The computations have been performed with the Grid [15–17] and Hadrons [18] software packages.

We use the same simulation parameters RBC/UKQCD is using in the heavy-light meson projects on exclusive semileptonic $B_{(s)}$ meson decays [19–22]. In particular, the valence-strange quark is simulated using DWF, whereas the valence-charm quark is simulated by using the Möbius DWF action [23, 24]. Their masses are tuned such that mesons containing bottom, charm and strange valence quarks have masses close to the physical ones. The physical bottom quark cannot currently be simulated with DWF and some EFT-based action is required: the b quark has been simulated at its physical mass using the Columbia formulation of the relativistic-heavy-quark (RHQ) action [25, 26], which is based on the Fermilab heavy quark action [27].

For the computation we average over 120 statistically independent gauge configurations, and on each configuration the measurements are performed on 8 different linearly spaced source-time planes. We use $\mathbb{Z}_2$ wall sources [28–30] to improve the signal. We compute 8 different momenta linearly spaced in $\boldsymbol{q}^2$ to cover the full kinematic range and another 2 momenta to increase the resolution for small $\boldsymbol{q}^2$. These have been induced through partially twisted boundary conditions [31, 32] for the charm quark with the same momentum in all three spatial directions.

6. Results

We now present some of the main findings of this study. For all the observables we report results from the two reconstruction approaches at values $\omega_0 = 0$ and $\omega_0 = 0.9\omega_{\text{min}}$. For the Backus-Gilbert method, we employ two different choices for the polynomial basis, namely exponentials $b_j(\omega) = e^{-j\omega}$ or shifted Chebyshev polynomials $b_j(\omega) = \tilde{T}_j(\omega)$.

In Fig. 2 we show the results for the quantity $\bar{X}(\boldsymbol{q}^2)$ (left) together with the effect of the variance reduction (right) outlined in Sec. 4. In particular, the latter shows that the reduction of the statistical error is substantial and it therefore emphasises the importance of regularisation methods for the final result. All the methods are in agreement, and the only deviation is associated with the different values of ω_0 as $\boldsymbol{q}^2$ increases. This is understood in terms of the different quality of the approximation as the phase space in ω shrinks, as illustrated in Fig. 1, and has to be taken into account in the systematics.

PoS(LATTICE2023)236

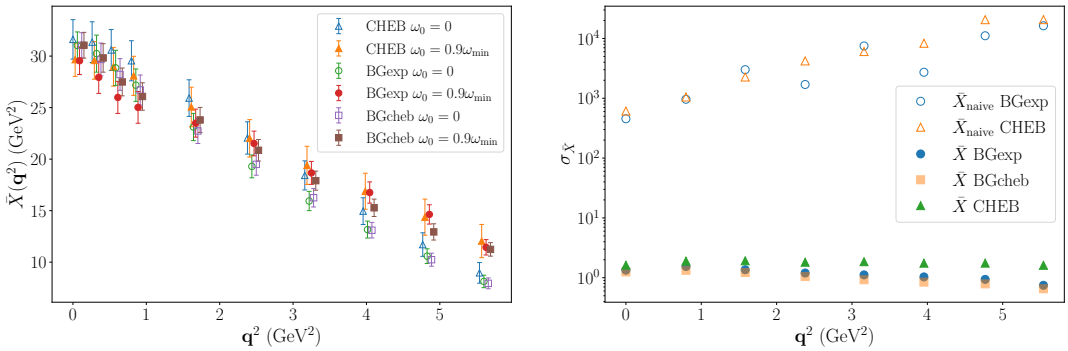

Figure 2: Left: estimate of $\bar{X}(\boldsymbol{q}^2)$ with the two different strategies for 10 different values of $\boldsymbol{q}^2$ with $N = 9$ and $\boldsymbol{q}_{\text{max}} = 5.83\,\text{GeV}^2$. Right: effect of the variance reduction to $\bar{X}_{\text{naive}}(\boldsymbol{q}^2)$ from the correction $\delta\bar{X}(\boldsymbol{q}^2)$ for the case $\omega_0 = 0.9\omega_{\min}$. The y axis shows the standard deviation $\sigma_{\bar{X}}$ for $\bar{X}_{\text{naive}}(\boldsymbol{q}^2)$ (empty symbols) and $\bar{X}(\boldsymbol{q}^2) = \bar{X}_{\text{naive}}(\boldsymbol{q}^2) + \delta\bar{X}(\boldsymbol{q}^2)$ (filled symbols).

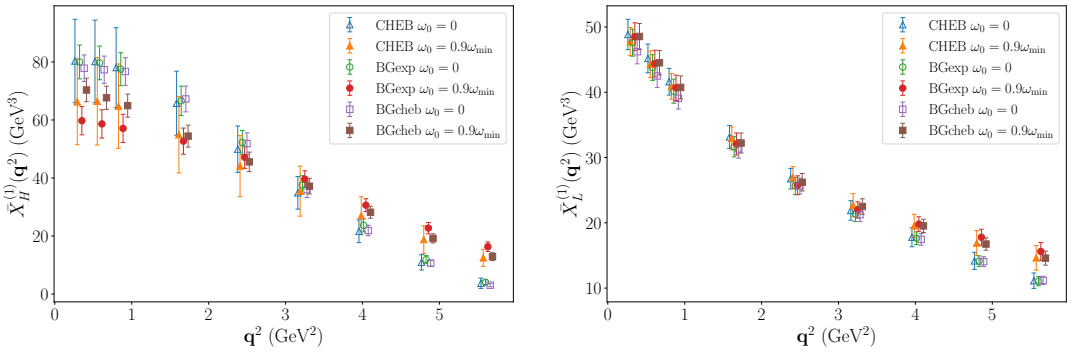

Figure 3: Evaluation of the numerators $\bar{X}_H^{(1)}(\boldsymbol{q}^2)$ (left) and $\bar{X}_L^{(1)}(\boldsymbol{q}^2)$ (right) of the hadronic mass and lepton differential moments at $n = 1$, respectively.

In Fig. 3 we show some of the results for the moments. In particular, we focus on the numerators $\bar{X}_H^{(n)}(\boldsymbol{q}^2)$ and $\bar{X}_L^{(n)}(\boldsymbol{q}^2)$ that enter the definition of the hadronic mass and lepton moments at order $n = 1$, as in the general expression Eq. (6). As for the decay rate, we see excellent agreement among the different methods. Note that, compared to the decay rate, the errors are larger for $\bar{X}_H^{(1)}(\boldsymbol{q}^2)$ and smaller (or comparable) for $\bar{X}_L^{(1)}(\boldsymbol{q}^2)$. This can be understood in terms of the differences of the kernels: indeed, the hadronic mass moments introduce extra factors that depend on ω in the kernels, whereas the behaviour of the leptonic kernels is smooth. We therefore expect the polynomial approximation to be more efficient in this second case.

7. Summary and outlook

We presented our results for a pilot study of B_s-meson inclusive semileptonic decays [5] highlighting the general setup for the calculation. In particular, we provide an extended framework that incorporates two different methods, one exploiting Chebyshev polynomials, and one exploiting

PoS(LATTICE2023)236

the Backus-Gilbert approach. We showed that the two are compatible for both the computation of the decay rate and the moments, and outlined how the two regularise the calculation of the observables to reduce the statistical noise, either acting on the data (Chebyshev) or modifying the coefficients of the polynomial approximation (Backus-Gilbert).

We also tested our setup to address some of the quantities related to hadronic mass and lepton energy moments, similarly to what was done in [6]. A full treatment of (differential) moments on the lattice will allow to compare with analytical OPE approaches and will provide a common ground to cross-validate different approaches. Moreover, moments do not depend on the CKM-matrix elements, and lattice calculations may allow to extract some of the parameters that appear in the perturbative expansion.

Overall, our work provides a solid foundation for future studies of semileptonic inclusive decays. However, several aspects require further investigations and will be the subject of future studies, in particular systematic errors associated with the polynomial approximation [33], finite-volume effects, discretisation errors, and the continuum limit.

Acknowledgments

This work used the DiRAC Extreme Scaling service at the University of Edinburgh, operated by the Edinburgh Parallel Computing Centre on behalf of the STFC DiRAC HPC Facility (www.dirac.ac.uk). This equipment was funded by BEIS capital funding via STFC capital grant ST/R00238X/1 and STFC DiRAC Operations grant ST/R001006/1. DiRAC is part of the National e-Infrastructure.

The works of S.H. and T.K. are supported in part by JSPS KAKENHI Grant Numbers 22H00138 and 21H01085, respectively, and by the Post-K and Fugaku supercomputer project through the Joint Institute for Computational Fundamental Science (JICFuS).

References

[1] M. T. Hansen, H. B. Meyer and D. Robaina, *Phys. Rev. D* **96** (2017) 094513 [1704.08993].

[2] S. Hashimoto, *Progress of Theoretical and Experimental Physics* **2017** (2017) 53 [1703.01881].

[3] P. Gambino and S. Hashimoto, *PHYSICAL REVIEW LETTERS* **125** (2020) 32001 [2005.13730].

[4] A. Barone, A. Jüttner, S. Hashimoto et al., *PoS* **LATTICE2022** (2023) 403 [2211.15623].

[5] A. Barone, S. Hashimoto, A. Jüttner et al., *JHEP* **07** (2023) 145 [2305.14092].

[6] P. Gambino, S. Hashimoto, S. Mächler et al., *JHEP* **07** (2022) 083 [2203.11762].

[7] J. C. A. Barata and K. Fredenhagen, *Commun. Math. Phys.* **138** (1991) 507.

[8] A. Weiße, G. Wellein, A. Alvermann et al., *Rev. Mod. Phys.* **78** (2006) 275 [cond-mat/0504627].

PoS(LATTICE2023)236

[9] G. Backus and F. Gilbert, *Geophysical Journal of the Royal Astronomical Society* **16** (1968) 169.

[10] M. Hansen, A. Lupo and N. Tantalo, *Physical Review D* **99** (2019) [1903.06476].

[11] Y. Shamir, *Nuclear Physics, Section B* **406** (1993) 90 [hep-lat/9303005v1].

[12] V. Furman and Y. Shamir, *Nuclear Physics, Section B* **439** (1994) 54 [hep-lat/9405004v2].

[13] Y. Iwasaki, 1111.7054.

[14] C. Allton, D. J. Antonio, Y. Aoki et al., *Physical Review D - Particles, Fields, Gravitation and Cosmology* **78** (2008) [0804.0473].

[15] P. Boyle, A. Yamaguchi, G. Cossu et al., "Grid: Data parallel C++ mathematical object library." https://github.com/paboyle/Grid.

[16] P. A. Boyle, G. Cossu, A. Yamaguchi et al., *PoS* **LATTICE2015** (2016) 023 [1512.03487].

[17] A. Yamaguchi, P. Boyle, G. Cossu et al., *PoS* **LATTICE2021** (2022) 035 [2203.06777].

[18] A. Portelli, R. Abott, N. Asmussen et al., *aportelli/hadrons: Hadrons v1.3*, Mar., 2022. 10.5281/zenodo.6382460.

[19] J. M. Flynn, R. C. Hill, A. Jüttner et al., *PoS* **LATTICE2018** (2019) 290 [1903.02100].

[20] J. Flynn, R. Hill, A. Jüttner et al., *PoS* **LATTICE2019** (2019) 184 [1912.09946].

[21] J. Flynn, R. Hill, A. Juettner et al., *PoS* **LATTICE2021** (2022) 306 [2112.10580].

[22] J. M. Flynn, R. C. Hill, A. Jüttner et al., 2303.11280.

[23] Y.-G. Cho, S. Hashimoto, A. Jüttner et al., *JHEP* **05** (2015) 072 [1504.01630].

[24] R. C. Brower, H. Neff and K. Orginos, *Comput. Phys. Commun.* **220** (2017) 1 [1206.5214].

[25] N. H. Christ, M. Li and H.-W. Lin, *Phys. Rev. D* **76** (2007) 074505 [hep-lat/0608006].

[26] H. W. Lin and N. Christ, *Physical Review D - Particles, Fields, Gravitation and Cosmology* **76** (2007) [hep-lat/0608005].

[27] A. X. El-Khadra, A. S. Kronfeld and P. B. Mackenzie, *Physical Review D - Particles, Fields, Gravitation and Cosmology* **55** (1997) 3933 [hep-lat/9604004].

[28] UKQCD collaboration, M. Foster and C. Michael, *Phys. Rev. D* **59** (1999) 074503 [hep-lat/9810021].

[29] UKQCD collaboration, C. McNeile and C. Michael, *Phys. Rev. D* **73** (2006) 074506 [hep-lat/0603007].

[30] P. A. Boyle, A. Juttner, C. Kelly et al., *JHEP* **08** (2008) 086 [0804.1501].

PoS(LATTICE2023)236

[31] G. M. de Divitiis, R. Petronzio and N. Tantalo, *Phys. Lett. B* **595** (2004) 408 [hep-lat/0405002].

[32] C. T. Sachrajda and G. Villadoro, *Phys. Lett. B* **609** (2005) 73 [hep-lat/0411033].

[33] R. Kellermann, A. Barone, S. Hashimoto et al., *PoS* **LATTICE2022** (2023) 414 [2211.16830].

PoS(LATTICE2023)236